Pupil-aware Holographic Display with Continuous Eyebox Expansion under Multi-Angle Illumination

*Yiqing Tao[1], Pengfei Mi[1], Xiangyu Meng[2], Wenbin Zhou[2], Yifan Peng[2], Xinxing Xia[1, *]*

[1] School of Mechatronic Engineering and Automation, Shanghai University, China

[2] Department of Electrical and Electronic Engineering, University of Hong Kong, Hong Kong SAR, China

(*Corresponding Author: lygxia@gmail.com)

Abstract

Holography offers natural three-dimensional depth perception through wavefront reconstruction. However, achieving a balance between the field of view (FOV) and the eyebox remains a challenge. In this study, we propose a novel approach using multi-angle illumination to enable continuous eyebox expansion, while employing filterless optics to miniaturize the near-eye display. To support this, we introduce the Pupil-HOGD-MI algorithm, which accounts for non-idealities in filterless near-eye displays by incorporating higher-order diffraction effects and pupil-aware optimization for multi-angle illumination. We validate our approach using a dual-angle holographic display prototype, demonstrating horizontal eyebox expansion alongside high image quality.

Author Keywords

Holographic near-eye display; eyebox expansion; pupil-aware.

1. Introduction

Holographic displays offer a groundbreaking approach to visualizing three-dimensional (3D) data. However, their performance is significantly constrained by the space-bandwidth product (SBP) of current devices, leading to limitations such as a narrow field of view (FOV) and a small eyebox [1]. To address these challenges, various strategies, including exit-pupil replication and scanning have been explored. Recent studies have demonstrated substantial improvements in eyebox size by utilizing lens array-based holographic optical elements (HOEs) and leveraging the higher-order diffraction properties of spatial light modulators (SLMs) [2].

Recent studies have investigated the use of multi-angle illumination as a promising method for expanding the eyebox in holographic displays. Simultaneous multi-angle illumination enhances the angle of emitted light, thereby increasing the étendue. This approach generates a greater number of viewpoints, which is directly proportional to the expansion of the eyebox [3]. Achieving this advanced illumination technique relies on time-multiplexing and custom beam deflection components. Additionally, it can be effectively implemented by combining coherent multi-angle illumination with optimized holographic techniques, further enhanced by integrating multiple laser diodes. This integration significantly alleviates the diffraction constraints of SLMs.

Moreover, the deployment of various incoherent light sources in conjunction with diverse light modulation devices has been extensively applied to both enhance the eyebox and reduce speckle noise [4]. However, challenges remain. When the pupil of the human eye exceeds the distance between individual viewpoints, multiple viewpoints can enter the pupil simultaneously, resulting in overlapping images on the retina. Therefore, it is critical to explore methods for achieving a continuously expanded eyebox using multi-angle illumination while addressing these overlapping image artifacts.

The core of the holographic display technique lies in the generation of holograms, with the hologram generation algorithm playing a pivotal role in determining the quality of the reconstructed image. A pupil-aware holographic display strategy can be achieved by incorporating the pupil model into the optimization algorithm [5]. Additionally, achieving a compact and portable holographic display requires minimizing the reliance on unnecessary optical components. By eliminating filtering optical elements and instead modeling higher-order diffractions directly within the hologram generation process, this software-centric approach reduces hardware dependency while enhancing the intelligence and efficiency of the display system [6].

This study proposes a novel approach that integrates multi-angle illumination with pupil-aware hologram optimization to achieve a continuous eyebox and improved performance. Hardware implementation employs multiple light sources for simultaneous multi-angle illumination, eliminating the need for filtering systems. A variable aperture camera simulates the human eye's pupil and retina. On the algorithmic side, we developed a wave propagation formula based on angular spectrum rotation, incorporating pupil constraints and higher-order diffraction effects into the hologram optimization process. The proposed method is validated through a dual-angle holographic near-eye display prototype.

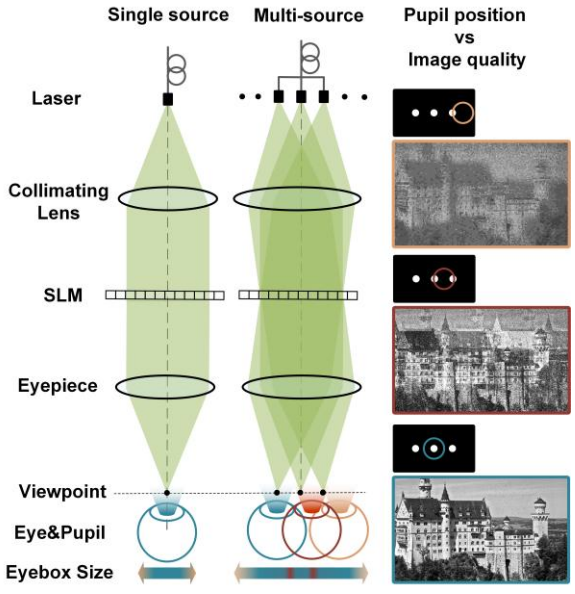

Figure 1. Schematic diagram of eyebox expansion with multi-angle illumination. Depending on the number of light sources to generate the corresponding viewpoints, eyebox size increases.

ISSN 0097-996X/25/5602-0707-$1.00 © 2025

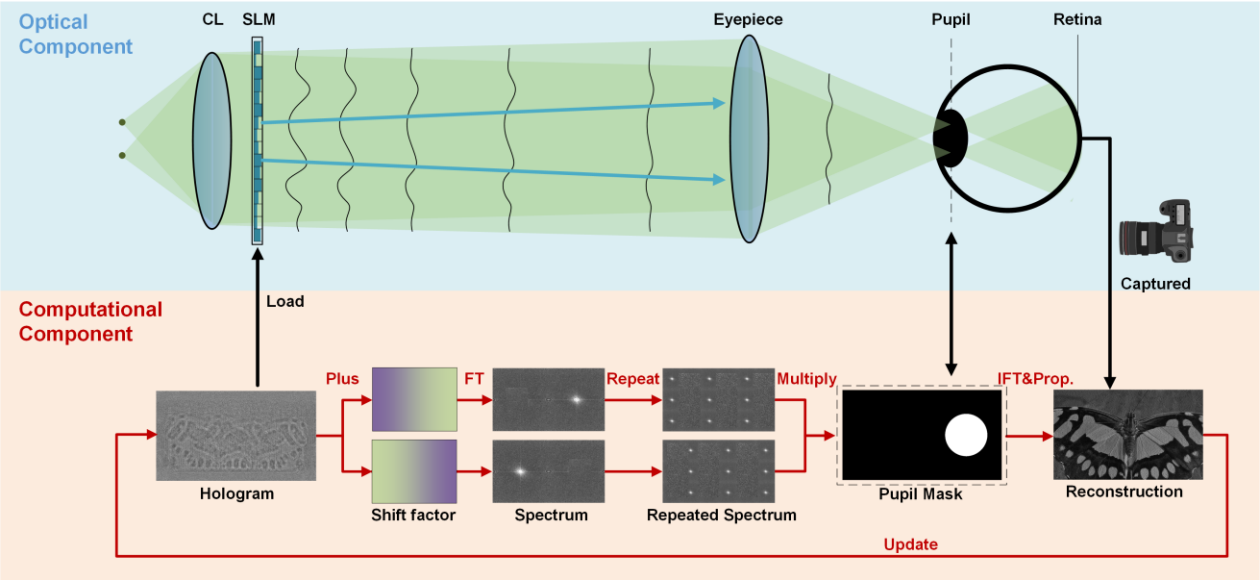

Figure 2. Overview of the proposed holographic near-eye display under multi-angle illumination and the Pupil-HOGD-MI algorithm. Top: The optical propagation path, with a dual light source as an example. Bottom: The algorithm computational path, simulates a forward propagation flow that incorporates off-axis propagation, higher-order diffractions and pupil filtering, and the ideal hologram is finally iterated using the gradient descent method.

2. Method

Figure 1 illustrates the strategy for achieving an expanded eyebox using a multi-angle illumination system. The system comprises lasers, a collimating lens (CL), a beam splitter (BS), an SLM, and an eyepiece. Unlike single-angle illumination, the laser array provides simultaneous illumination from multiple angles to the SLM, which generates a series of distinct viewpoints. The approach significantly expands the eyebox of the holographic display.

The visibility of holographic images from different light sources depends on the pupil's position and movement. When the spacing between adjacent viewpoints exceeds the pupil's diameter, only one viewpoint enters the pupil at a time, resulting in a sharp holographic image on the retina. However, as the pupil approaches the edge of a viewpoint, image quality decreases significantly. Conversely, if the spacing between viewpoints is smaller than the pupil's diameter, multiple viewpoints can overlap within the pupil, causing image aliasing. To address this aliasing in scenarios with closer viewpoint spacing, we developed an advanced propagation framework for multi-angle illumination. This framework dynamically adjusts to changes in pupil position and size, ensuring consistent image quality across all viewpoints.

Among various hologram optimization algorithms, the stochastic gradient descent (SGD) algorithm is widely used for its simplicity and effectiveness [7]. However, display quality is also impacted by hardware limitations, such as unwanted higher-order diffractions during reconstruction. To maintain a compact display design, we employ an unfiltered holography optimization approach, the Higher-Order Gradient Descent (HOGD) algorithm, which simulates and compensates for higher-order diffractions during the optimization [6].

The human eye's pupil acts as a dynamic low-pass filter, and integrating eye tracking into hologram generation algorithms enables pupil-aware optimization, improving display efficiency. This approach is implemented in the Pupil-HOGD algorithm, which we further extend into the Pupil-HOGD under multi-angle illumination (Pupil-HOGD-MI) algorithm. Figure 2 illustrates the proposed concept for a holographic near-eye display under dual light sources and the Pupil-HOGD-MI framework. Initially, an initialized hologram is loaded onto the SLM, which is iteratively updated throughout the optimization process. With off-axis illumination, the same SLM region simultaneously modulates off-axis light beams from multiple directions.

To accurately model the physical propagation of off-axis light waves between parallel planes, the computational process must reflect the actual propagation behavior. On the SLM plane, the light field is pre-shifted according to the tilt angle of each illumination beam.

$$\hat{\varphi}_k = \exp\left\{ i \frac{2\pi}{\lambda} \left(x \sin\theta_{x_k} + y \sin\theta_{y_k} \right) \right\} \tag{1}$$

For each beam, a tilt factor $\hat{\varphi}_k$ corresponding to its tilt angle is introduced to create the required offset, simulating the effect of tilted parallel light beams and generating an offset light field, $u(x, y)$.

$$u_{\text{unfilt}} = \sum_{i,j=-(\alpha-1)/2}^{(\alpha-1)/2} \mathcal{F}\{u(x,y)\}\left(f_x + \frac{i}{p}, f_y + \frac{j}{p} \right) \tag{2}$$

The offset light fields from multiple light sources propagate forward simultaneously along the optical path and are processed in parallel within the algorithm. In the optical system, the absence of a filtering component naturally results in the production of a higher-order spectrum in the Fourier plane due to the Fourier lens. Computationally, the spectral distribution is obtained through the Fourier transform (FT), forming two distinct spectral centers, each corresponding to one of the angular light sources.

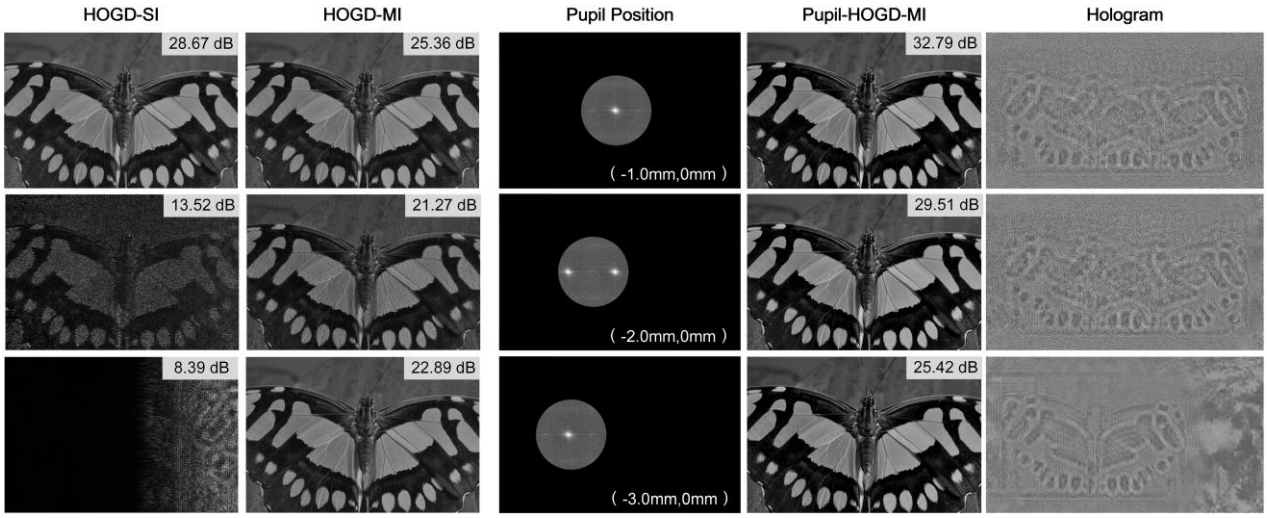

Figure 3. Simulation results. Left: Comparison of eyebox condition between HOGD-SI and HOGD-MI algorithm; Right: The reconstructed image of Pupil-HOGD-MI and corresponding holograms and pupil positions.

In the absence of a filtering system, the propagation function is modified to simulate the higher-order diffraction effects of the SLM. The light field on the SLM plane is replicated in the frequency domain, with the finite square pixel spacing attenuating these replicas through a two-dimensional *Sinc* function.

$$M(x,y)=\begin{cases}1 & \text{if } |l-D(x,y)|<D_p\\ 0 & \text{otherwise}\end{cases} \tag{3}$$

Optically, the pupil is positioned at the spectral plane where the light rays converge, acting as a low-pass filter to block unfiltered higher-order diffracted light. Computationally, the pupil function $M(x, y)$ is used to optimize the phase. For a pupil diameter D_p and an eyepiece focal length F, $M(x, y)$ functions as a circular filter in the Fourier domain, with an inner value of 1 and 0 elsewhere.

By accurately simulating optical forward propagation, the algorithm optimizes the hologram iteratively, accounting for realistic non-ideal factors. After computed forward propagation, the reconstructed amplitude is compared with the target amplitude, and the hologram is incrementally refined using the gradient descent method [7].

3. Experiments and Results

The Pupil-HOGD-MI method modifies forward propagation to account for phase shifts from multi-angle illumination, hardware-induced filtering, and higher-order diffraction effects. To evaluate its ability to integrate pupil effects and higher-order diffraction, simulation experiments were conducted using three hologram optimization methods: HOGD under single-angle illumination (HOGD-SI), HOGD under multi-angle illumination (HOGD-MI), and Pupil-HOGD-MI.

The simulations employed dual-angle illumination with angles of ($\pm 0.7°$, 0°). The pupil diameter was set to 3 mm, with the pupil positions at (-1.0mm, 0mm), (-2.0mm, 0mm), and (-3.0mm, 0mm). The distance between the SLM and the target plane was maintained at 80 mm. Results are shown in Fig. 3.

The first and second columns of Fig. 3 compare the reconstructions under varying illumination conditions and pupil positions using the HOGD algorithm. With the HOGD-SI method, the image quality is relatively high at the central position but diminishes significantly at (-2.0mm, 0mm), indicating a limited eyebox. In contrast, the HOGD-MI method maintains clear images across the pupil range from (-1.0mm, 0mm) to (-3.0mm, 0mm), demonstrating the improved eyebox capability of multi-source illumination. However, at (-2.0mm, 0mm) image quality slightly degrades as the pupil simultaneously captures both light beams.

The fourth, fifth, and sixth columns of Fig. 3 highlight the optimization performance of the Pupil-HOGD-MI algorithm. The third column shows the pupil position and its filtering effect, while the fourth column displays the reconstruction results, where a clear improvement in image quality is evident. The fifth column presents the optimized holograms at different pupil positions. The Pupil-HOGD-MI algorithm incorporates pupil aperture modeling and, despite wavefront shift and information loss in the frequency domain due to multi-angle illumination delivers superior image quality across all pupil positions.

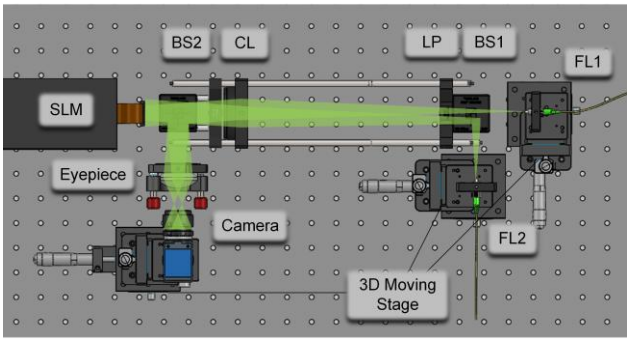

Figure 4. Bench-top system of holographic near-eye display under multi-angle illumination.

To validate the proposed method and simulations, we constructed an experimental prototype using laser light sources at two angles, as shown in Fig. 4. The hardware setup includes a laser source (MGL-III-532-50mW) coupled to two distinct laser fiber outputs via a fiber coupler (Thorlabs PN530R51). A SLM (UPOlabs HDSLM64R, 1,920×1,080 resolution, 6.4 μm pitch) is

illuminated. After passing through the collimating lens, the light emerges as dual-angle illumination. The camera and the two fibers are mounted on a 3D moving stage, respectively. The system's software is powered by a Nvidia RTX 3090 graphics card. To reduce memory usage, the content for each lighting condition is optimized sequentially. Utilizing the Pupil-HOGD-MI algorithm, a single phase pattern is generated on the PC, with the computational process taking approximately 4 minutes for 500 iterations.

Figure 5 shows the results of the HOGD-MI and Pupil-HOGD-MI experiments conducted with dual light sources. Butterfly patterns were recorded with the camera lens aperture, representing the pupil, centered at positions (-1mm, 0mm), (-2mm, 0mm), and (-3mm, 0mm). The high image quality observed at each position highlights the feasibility of the proposed multi-light source holographic near-eye display for achieving continuous pupil dilation, while also validating the accuracy and effectiveness of the Pupil-HOGD-MI algorithm in simulating physical light propagation.

Notably, at position (-2mm, 0mm), simultaneous illumination from both light sources does not cause image aliasing, thanks to the algorithm's effective optimization. Additionally, the incorporation of pupil filtering and its role in constraining the optimization process enables the Pupil-HOGD-MI algorithm to consistently deliver superior image quality across all positions compared to the HOGD-MI algorithm.

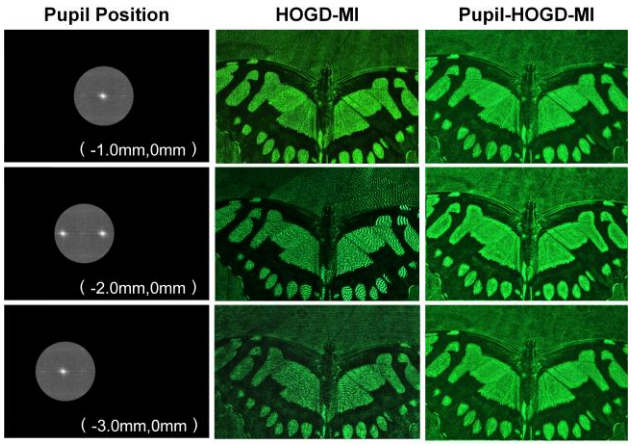

Figure 5. Experimental results. Left: spectral information under the pupil mask; Middle: captured images at different pupil positions using HOGD-MI; Right: captured images at different pupil positions using Pupil-HOGD-MI.

4. Conclusion

This study presents a novel approach to improving holographic near-eye displays by expanding the eyebox and enhancing image quality using multi-angle illumination and the pupil-aware algorithm. These advancements are validated on the bench-top prototype, paving the way for more immersive visual experiences. Future work should focus on fast hologram generation with robust eye-tracking, full-color 3D displays, and compact designs with expanded FOV using off-axis HOE combiners. Key directions include developing lightweight neural networks for real-time CGH, integrating RGB lasers for color, and designing optical systems to achieve a wider FOV and a reduced form factor for eyeglass-style displays.

5. Acknowledgements

This research was supported by the Science and Technology Commission of Shanghai Municipality (24511106502, 20ZR1420500), the National Key Research and Development Program of China (2021YFB2802200), the National Natural Science Foundation of China (62322217, 62005154), and the Research Grants Council of Hong Kong (ECS 27212822, GRF 17208023).

6. References

1. Xia X, Guan Y, State A, Chakravarthula P, Cham TJ, Fuchs H. Towards Eyeglass-style Holographic Near-eye Displays with Statically Expanded Eyebox. 2020 IEEE International Symposium on Mixed and Augmented Reality (ISMAR); 2020; pp. 312-319. Available from: https://doi.org/10.1109/ISMAR50242.2020.00057
2. Jo Y, Yoo C, Bang K, Lee B, Lee B. Eye-box extended retinal projection type near-eye display with multiple independent viewpoints. Applied Optics. 2021;60(4):A268-A276. Available from: https://doi.org/10.1364/AO.408707
3. Chao B, Gopakumar M, Choi S, Kim J, Shi L, Wetzstein G. Large Étendue 3D Holographic Display with Content-adaptive Dynamic Fourier Modulation. SIGGRAPH Asia 2024 Conference Papers; 2024; 26:1-12. Available from: https://doi.org/10.1145/3680528.3687600
4. Kuo G, Waller L, Ng R, Maimone A. High resolution étendue expansion for holographic displays. ACM Transactions on Graphics. 2020;39(4), 66:1-14. Available from: https://doi.org/10.1145/3386569.3392414
5. Chen T, Wang Z, Wang Y, Feng Q, Lv G. Multiple viewpoints optimization for holographic near-eye display based on a pupil mask. Optics & Laser Technology; 2024; 179:111400. Available from: https://doi.org/10.1016/j.optlastec.2024.111400
6. Kim J, Gopakumar M, Choi S, Peng Y, Lopes W, Wetzstein G. Holographic Glasses for Virtual Reality. ACM SIGGRAPH 2022 Conference Proceedings; 2022; 33:1-9. Available from: https://doi.org/10.1145/3528233.3530739
7. Peng Y, Choi S, Padmanaban N, Wetzstein G. Neural holography with camera-in-the-loop training. ACM Trans. Graph.; 2020 Nov; 39(6):185:1-14. Available from: https://doi.org/10.1145/3414685.3417802